Surface and Subsurface Oxidation of Mo_2C/Mo(100): Low-Energy Ion-Scattering, Auger Electron, Angle-Resolved X-Ray Photoelectron, and Mass Spectroscopy Studies

László Óvári, János Kiss,* Arnold P. Farkas, and Frigyes Solymosi

Reaction Kinetics Research Group of the Hungarian Academy of Sciences, University of Szeged, P.O. Box 168, H-6701 Szeged, Hungary

Received: September 22, 2004; In Final Form: December 22, 2004

The interaction of oxygen with a carburized Mo(100) surface was investigated at different temperatures (300−1000 K). The different information depths of low-energy ion-scattering (LEIS) spectroscopy, with topmost layer sensitivity, Auger electron spectroscopy (AES), and angle-resolved X-ray photoelectron spectroscopy (ARXPS) allowed us to discriminate between reactions on the topmost layer and subsurface transformations. According to ARXPS measurements, a carbide overlayer was prepared by the high-temperature decomposition of C_2H_4 on Mo(100), and the carbon distribution proved to be homogeneous with a Mo_2C stoichiometry down to the information depth of XPS. O_2 adsorbs dissociatively on the carbide layer at room temperature. One part of the chemisorbed oxygen is bound to both C and Mo sites, indicated by LEIS. Another fraction of oxygen atoms probably resides in the hollow sites not occupied by C. The removal of C from the outermost layer by O_2, in the form of CO, detected by mass spectroscopy (MS), was observed at 500−600 K. The carbon-depleted first layer is able to adsorb more oxygen compared to the Mo_2C/Mo(100) surface. Applying higher doses of O_2 at 800 K results in the inward diffusion of O and the partial oxidation of Mo atoms. This process, however, is not accompanied by the removal of C from subsurface sites. The depletion of C from the bulk starts only at 900 K (as shown by MS, AES, and XPS), very probably by the diffusion of C to the surface followed by its reaction with oxygen. At $T_{ads} = 1000$ K, the carbon content of the sample, down to the information depth of XPS, decreased further, accompanied by the attenuation of the C concentration gradient and a substantially decreased amount of oxygen.

1. Introduction

Transition metal carbides are in the focus of intensive research for several reasons. Their outstanding mechanical properties are well-known. In the field of nanoelectronics, low-resistance ohmic contacts between carbon nanotubes and metal substrate can be achieved through metal carbide junctions.[1] Carbides and nitrides of molybdenum are of interest for diffusion barriers and protective coatings.[2] Moreover, transition metal carbides are good catalysts in several reactions and have similar electronic properties to those of platinum metals, so they may substitute for expensive noble metals in some hydrogenation, dehydrogenation, and hydrodesulfurization reactions.[3−5] CH_4 and other hydrocarbons can be transformed into aromatics with high selectivity on zeolite-supported Mo_2C catalysts.[6−8] The interaction of O_2 with Mo_2C is an important issue in any application when the carbide is in contact with air and is interesting from the catalytic point of view, because molybdenum carbide is generally prepared from MoO_3 and also because molybdenum oxycarbides are very selective in the isomerization of paraffins.[9]

The formation and structure of carbon overlayers, generally prepared by the decomposition of C_2H_4 or other hydrocarbons on group IVB−VIB transition metals, were the subject of intensive research.[5] The Mo(100) surface at low temperature (5−600 K) could be saturated with C up to the coverage of $\Theta = 1$ monolayer (ML) through different intermediate structures (c(2 × 2) at $\Theta = 0.5$ ML and a zigzag structure at $\Theta = 0.67$ ML).[10,11] Annealing to $T \geq 800$−1000 K led to subsurface migration of C.[12−14] Near-edge X-ray absorption fine structure (NEXAFS) spectroscopy and quantitative mass spectroscopy (MS) results showed that a relatively thick carbide layer containing several monolayers of carbon can be produced from C_2H_4 on Mo(100) and Mo(110) by high-temperature adsorption/annealing.[12,15]

High-temperature carburization produced complex low-energy electron-diffraction (LEED) patterns especially at high carbon coverages on Mo(111),[13] Mo(110),[14] W(100),[16] and other surfaces of IVB−VIB group elements, assigned generally to surface reconstruction. The Mo(100) surface may be an exception because in LEED measurements no significant reconstruction was assumed.[10,11,17] Angle-resolved low-energy ion-scattering (LEIS) spectroscopy measurements[18] and tensor LEED results[17] showed that C atoms of the first layer reside in the four-fold hollow sites in both superficial carbon structures and three-dimensional (3D) carbide overlayers on Mo(100). Subsurface C atoms are believed to reside in the interstitial sites of the metal lattice, but detailed crystallographic studies on carbide overlayers are lacking at present as well as the knowledge of the C concentration profile.

The interaction of oxygen with molybdenum surfaces was also investigated in detail. At low temperatures up to 300 K, the presence of O adsorbed on bridge sites, (quasi) three-fold hollow sites, and at higher exposures on-top O was observed by high-resolution electron energy-loss spectroscopy (HREELS) on Mo(111)[19] and Mo(110),[20] depending on the orientation of the surface. O atoms bound to three-fold and on-top sites were identified during high-temperature oxidation of Mo(111), Mo(110), and Mo(100).[19−21] The 3D oxide formation on all of

* Author to whom correspondence should be addressed. Phone: +36-62-544-803. Fax: +36-62-420-678. E-mail: jkiss@chem.u-szeged.hu.

10.1021/jp045693a CCC: $30.25
Published on Web 02/17/2005

these surfaces was accompanied by the relative increase in the number of on-top O. High-temperature oxidation of the Mo(100) surface proceeds through intermediate structures characterized by different reconstructions.[21] The Mo(112) surface is suitable for the preparation of epitaxial MoO_2 layers.[22−24]

X-ray photoelectron spectroscopy (XPS) proved to be an efficient tool for the determination of the oxidation states of molybdenum and also for obtaining information on the oxide layer thickness.[24−29] The onset of the formation of a thick MoO_2 oxide layer depends on the adsorption temperature. At T_{ads} = 713 K, 1×10^7 L of O_2 exposure was necessary for an extensive oxidation of the Mo(100) surface to a mainly MoO_2 state, with also some Mo^{VI}, while 6×10^4 L of O_2 was sufficient to obtain a similar result at T_{ads} = 873 K.[29] The formation of crystalline MoO_2 was proved by Raman spectroscopy, while the Mo^{VI} component was assigned to surface polymolybdate species.[29]

The interaction of oxygen with transition metal carbide surfaces was also investigated. Oxygen adsorbs dissociatively at 150−300 K on the α-Mo_2C(0001) surface.[30,31] Heating the carburized Mo(100) surface saturated with oxygen resulted in two CO desorption peaks at ∼900 and ∼1050 K.[12] The latter peak was assigned to the reaction of O with subsurface C. Only one desorption peak was found on Mo_2C(0001), but it was not followed above 950 K in that case.[31] Migration of O into the bulk of the carbide during heating was also assumed.[30,31] Supported Mo_2C catalysts could be oxidized to Mo^{IV}−Mo^{VI} states even with CO_2 at high pressure (1 bar).[32] In the presence of the K adlayer, the oxidation of a Mo_2C/Mo(100) sample by CO_2 occurred to a larger extent, which was explained by the formation of anionic CO_2^- and by its higher reactivity.[33]

Recently, we investigated the carburization of the Mo(100) surface by C_2H_4 adsorption at 900 K and annealing to 1265 K and also the high-temperature oxidation of the carbide up to 1265 K.[34] It was shown through the comparison of LEIS, Auger electron spectroscopy (AES), and XPS measurements that 3D carburization of the molybdenum surface does not proceed in a layer-after-layer mode, but C accumulates simultaneously in the first few layers. It does not exclude necessarily the existence of a gradient in the C concentration. With regards to the oxidation of the carbide layer, the comparison of the LEIS and AES results indicated that the consumption of C and the accumulation of O atoms initially take place in the first layer, but further oxidation leads to the C depletion of the deeper layers and the formation of subsurface O as well.

The aim of the present work was the characterization of the carburized Mo(100) surface with regards to the stoichiometry and the C concentration profile and also to get a more elaborate picture of its interaction with oxygen at both low and high temperatures. Special attention was paid to the migration of C and O perpendicular to the surface. The different surface sensitivity of LEIS, AES, and angle-resolved X-ray photoelectron spectroscopy (ARXPS) allowed us to obtain a certain depth profile of the sample. Detailed XPS measurements helped us determine changes in the oxidation states of Mo and C.

2. Experimental Section

The experiments were performed in an ultra-high-vacuum (UHV) system (base pressure 5×10^{-10} mbar), equipped with facilities for LEIS, AES, and XPS. LEIS spectra were obtained using the same Leybold EA10/100 hemispherical analyzer as for XPS and AES but with the polarity of the voltage biases inverted to detect He^+ ions. With all three methods, spectra were collected at 300 K sample temperature. AES was performed with a Vacuum Generators electron gun applying 2.5 keV electron energy and 5 V modulation. XPS measurements were carried out with a constant 50 eV pass energy, using an Al Kα X-ray anode. The sample could be tilted for angle-resolved measurements, but the anode and the analyzer were at fixed positions. The takeoff angle of the photoelectrons was measured with respect to the surface plane.

TABLE 1: Selected Characteristic Mo($3d_{5/2}$) Binding Energies

Mo^0	Mo_2C	Mo^{II}	Mo^{IV}	Mo^{V}	Mo^{VI}	ref
227.6	227.8					35
227.9	228.1					36
	227.7					37
	228.0					38
227.5		227.95				25
227.95		228.3				28
227.9			229.5[a]	231.1[a]		26
227.7			229.25[a]	230.9[a]		24
				231.6[b]		39
227.6			229.4[a]		232.6	40
		228.6[c]				41
			229.7[c]	230.8[c]	232.6	9

[a] In MoO_2. [b] In Mo_2O_5. [c] In MoO_xC_y.

A Specs IQE 12/38 ion source was used for LEIS. The primary energy was 800 eV. The incident angle (the angle between the ion beam and the surface plane) was 40°, while the mean scattering angle was 95°. Due to the ±10° acceptance angle of the analyzer in ion-scattering mode, direct recoil peaks, associated with surface atoms, ionized and sputtered off by He^+ ions in single collisions, were also present in the spectra at low kinetic energies.

A quadrupole mass spectrometer was used to analyze gas-phase products.

The areas of C(1s), O(1s), and Mo(3d) X-ray photoelectron (XP) peaks (doublet), areas of normal LEIS peaks (not direct recoil features), and peak-to-peak intensities of C KLL (271 eV) and O KLL (503 eV) AES transitions, referenced to the Mo MNN (221 eV) peak-to-peak intensity, were used to compare changes in the different surface layers.

The binding-energy scale for XPS was referenced to the position of the Mo($3d_{5/2}$) peak of the carbide, taken to be 227.95 eV. Carburization of a Mo metal surface induces only slight changes in the Mo(3d) feature; it results in a small upward shift (0.2 eV, Table 1). Scofield photoelectric cross sections were used for composition and coverage calculations,[42] applying the XPS Multiquant software. XP peaks were deconvoluted using asymmetric Gauss−Lorentz mix functions. A Shirley background was subtracted.[43] Coster−Kronig broadening of the Mo($3d_{3/2}$) peak was also taken into account.[44]

The Mo(100) single crystal was cleaned by heating in oxygen. This was followed by argon ion bombardment and annealing at 1500 K. Some oxygen remained on the surface after this procedure, but it could be removed almost completely during carburization.

The Mo(100) surface was carburized by repeating C_2H_4 adsorption (50 L) at 900 K and annealing in a vacuum to 1265 K, similar to the method of Schöberl,[12] until the C content reached saturation, monitored by LEIS, AES, and XPS. The characteristic three-lobe structure of the C KLL AES peak indicates the formation of carbidic (rather than graphitic or amorphous) C.

3. Results

3.1. Characterization of the Carbide Overlayer. The C(1s) region of the XP spectra of the carburized surface collected at

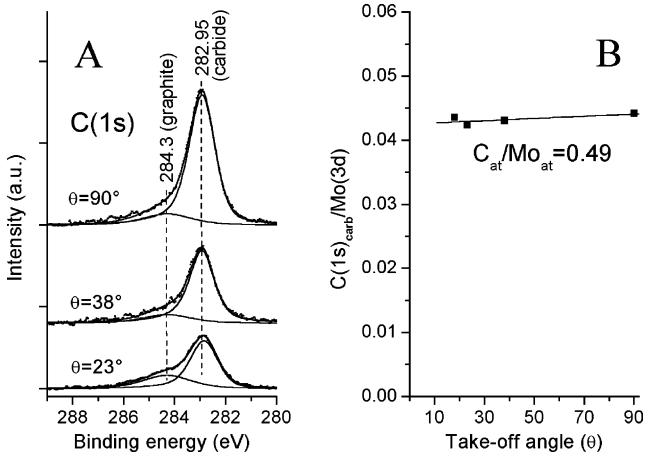

Figure 1. (A) C(1s) window of the X-ray photoelectron spectra of the carbide surface collected at different takeoff angles (θ). (B) Peak area ratio of the carbidic C(1s) component and the Mo(3d) doublet as a function of θ.

different takeoff angles (θ) are presented in Figure 1A. The C(1s) peak at normal detection was found at 282.95 eV, which is characteristic of carbides.[38] The C feature, however, had a small tail toward higher binding energies, which appeared as a shoulder at 284.3 eV when $\theta = 23°$ was applied, indicating that some graphite is also present on the surface. At low takeoff angles, a small, but reproducible, downward shift (~0.1 eV) of the carbon peak maximum was observed. This shift was a bit more evident when the carbide contribution was separated from the graphite shoulder by deconvolution. Reduction of θ resulted in a slight broadening of the carbidic component as well (the full width at half-maximum (fwhm) was 1.2 eV at $\theta = 90°$ and 1.3 eV at $\theta = 23°$). These changes indicate a somewhat different state of the first carbon layer. However, the position of the Mo(3d) doublet did not shift (or it was below the detection limit) at glancing emission.

The peak area ratio of the carbidic C(1s) component and the Mo(3d) doublet as a function of θ is presented in Figure 1B. Apparently it is independent of θ, which implies that C is dispersed homogeneously (with zero concentration gradient) in the crystal down to the information depth of XPS, estimated to be 5.7 nm at normal emission. On the basis of the homogeneity of the C distribution, the C/Mo atomic ratio was calculated to be 0.49, which means a Mo_2C stoichiometry. The information depth of XPS is only slightly different for C(1s) and Mo(3d) photoelectrons, because their kinetic energies are similar (1203 and 1258 eV, respectively). The C/Mo atomic ratio was, however, corrected also for this difference, using inelastic-mean-free-path (imfp) values obtained by the Gries equation.[45] In Mo metal, the imfp value at 1200 eV calculated by the Gries method (1.91 nm) agrees well with that obtained by Tanuma et al. (1.89 nm).[46] For the estimation of the information depth, the Gries equation was used. The imfp value at 1200 eV obtained this way for the parent metal is very similar to that of Mo_2C (1.91 nm) or MoO_2 (2.08 nm). The information depth was taken to be 3 times the imfp in the carbide.

Considering the fact that XPS gives averaged information of several layers, it cannot be excluded that the C/Mo atomic ratio of the topmost carbide layer is somewhat different.

3.2. Gas-Phase Products in the Interaction of Carbide with Oxygen. The removal of C by O_2 was first investigated following the $m/e = 28$ and 44 amu MS signals, characteristic of CO and CO_2, as a function of time, during O_2 adsorption at the given temperatures (Figure 2). The detailed experimental

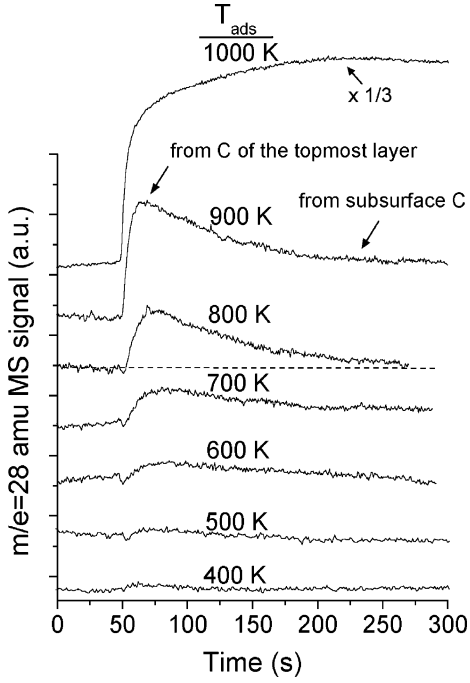

Figure 2. The $m/e = 28$ amu MS signal as a function of time *during* O_2 exposition on Mo_2C/Mo(100), followed isothermally. O_2 adsorption starts at 50 s, 300 s ≈ 20 L of O_2.

procedure was as follows. Oxygen was continuously admitted into the chamber through a capillary (started at 0 s). The sample was moved in front of the capillary at 50 s (the MS was not in line of sight in this position) and left there until the end of measurements. This method was chosen because Fukui et al.[47] assumed that nascent O atoms, formed in the chemisorption of O_2 on Mo_2C(0001), can react with surface C even at room temperature. Control measurements were also performed, repeating the same procedure but leaving the sample far from the capillary to determine the extent of CO desorption from the sample holder due to its warming and possible desorption of CO from the chamber wall due to the presence of O_2. This (small) contribution was subtracted from the curves obtained in "real" measurents. Measuring times more than 300 s were not possible, because of a larger CO desorption from the sample holder at high temperatures. The O_2 exposure up to 300 s corresponded to ~20 L.

At none of the adsorption temperatures examined was found any detectable change in the $m/e = 44$ amu signal, which means that the increase in the $m/e = 28$ amu signal corresponds to CO formation (desorption). A temperature of 500 K was the lowest at which CO formation could be unambiguously observed; a small, but well-reproducible, peak was found (Figure 2). A very small peak appeared even at 400 K; however, it cannot be excluded that a small amount of molecular CO on the surface (from the background) is displaced during O_2 adsorption and moved to the gas phase. No molecular CO is stable on our surface above 450 K.[48]

More significant CO formation takes place at higher adsorption temperatures. Up to $T_{ads} = 800$ K, the $m/e = 28$ amu signal reaches a maximum as a function of time and decreases to its original value up to the end of measurements, while at $T_{ads} \geq 900$ K it is stabilized at a higher level at $t = 300$ s. It suggests that CO can be produced in two mechanisms, one of which is significant only at higher temperatures. AES measurements (see below) showed that C/Mo relative intensity decreased by ~40% due to 20 L of O_2 exposure at 800 K. It means that a large amount of surface C (one carbon layer, as an order of

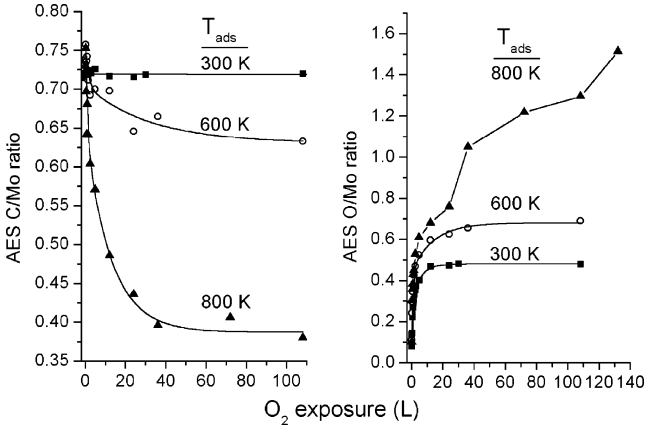

Figure 3. C/Mo and O/Mo AES relative intensities as a function of O_2 exposure on Mo_2C/Mo(100) at different temperatures.

TABLE 2: C/Mo Relative Intensities (Normalized to the Clean Carbide Surface) after 108 L of O_2 Adsorption at Different Temperatures

T (K)	AES	XPS ($\theta = 23°$)	XPS ($\theta = 90°$)
800	0.54	0.76	0.95
900	0.19	0.47	0.74
1000	0.40	0.49	0.63

magnitude) has been removed up to this point. The area under the $m/e = 28$ amu curve taken at $T_{ads} = 1000$ K, however, was 28 times higher than the area at 800 K, which requires several monolayers of C that can be provided only by the subsurface C reservoir in the sample. We feel safe to conclude that the plateaus observed from $T_{ads} = 900$ K in the MS curves can be assigned to the reaction of subsurface C with O. The maximum-type feature dominant at $T_{ads} \leq 800$ K is assigned to the reaction of O with C on the outermost layer. The reaction of subsurface carbon with oxygen is probably preceded by the migration of carbon up to the topmost layer.

3.3. Characterization of the Surface Interacting with Oxygen. C/Mo and O/Mo relative Auger intensities as a function of O_2 exposure at different temperatures are displayed in Figure 3. O_2 adsorption did not lead to the decrease in the C/Mo ratio at room temperature, but the consumption of C was observed at $T_{ads} = 600$ and 800 K (and even at $T_{ads} = 500$ K, not shown). With regards to the O/Mo ratio, it demonstrated a saturation behavior up to $T_{ads} = 600$ K, while its exposure dependence was more complex at $T_{ads} = 800$ K. After a rapid increase at low exposures, it nearly levels off up to 24 L, followed by a dramatic increase at 36 L. At even higher exposures up to 130 L, the O/Mo relative intensity continues to grow moderately.

The O/Mo relative Auger intensity after 108 L of O_2 adsorption at 900 K was similar to that obtained after the same oxygen dose at 800 K, while the C/Mo ratio was reduced to 0.14. Interestingly, raising the adsorption temperature to 1000 K led to an increase in the C/Mo intensity to 0.29, while the O/Mo Auger ratio decreased to 0.42 (for normalized C/Mo values see Table 2).

Ion-scattering spectra, collected after increasing O_2 exposures at room temperature, are presented in Figure 4A. Besides the peaks associated with He^+ ions scattered on atoms of the topmost layer in single collisions, recoil peaks (denoted by the subscript "r") can also be present in the spectra at low energies. O_2 adsorption led to the gradual enlargement of the O peak (484 eV) accompanied by a moderate attenuation of the Mo peak (729 eV) and the rapid decrease of the C peak (411 eV). At higher exposures, a new peak appeared at 44 eV. It was completely absent in the spectrum of the clean carbide surface,

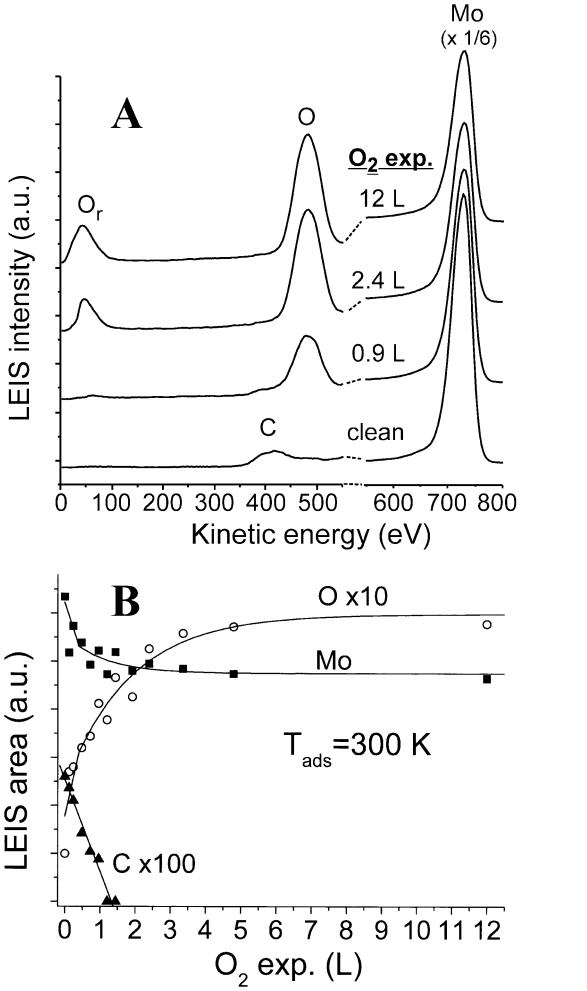

Figure 4. (A) LEIS spectra collected after increasing O_2 exposures at 300 K on Mo_2C/Mo(100) overlayer. (B) LEIS peak areas as a function of O_2 exposure on Mo_2C/Mo(100) at 300 K.

which strongly suggests that it does not belong to C or Mo atoms but to recoiled O. Ions sputtered off the surface in multiple collisions may also contribute to its intensity. LEIS peak areas as a function of O_2 exposure are displayed in Figure 4B.

Next, we examined with LEIS the adsorption of oxygen on Mo_2C/Mo(100) at and above 800 K. "Normal" and recoil oxygen peak areas obtained at 800 K adsorption are displayed as a function of exposure in Figure 5. Both are normalized to saturation at 300 K. The two curves show significant differences; at low exposures (up to ~5 L), peak O_r increases less steeply than peak O, but from 36 L a dramatic increase in the O_r intensity was observed (note that at the same exposure a step in the AES O/Mo curve was found). The intensity of the O LEIS peak, however, only slightly increased in the 36−132 L region. Mo LEIS area decreased linearly with the O area up to 36 L (see the inset of Figure 5). A break can be seen in the Mo−O curve at that point, and the Mo signal diminished significantly at slightly larger O peaks. Mo, O, and O_r LEIS intensities after 108 L of O_2 adsorption at 900 K were similar to those observed after the same oxygen dose at 800 K.

Saturation oxygen signals obtained by XPS, AES, and LEIS are displayed in Figure 6 as a function of adsorption temperature, normalized to saturation at 300 K. At $T_{ads} = 800$ K, oxygen intensities obtained after an O_2 dose slightly smaller than 36 L were taken into account in this curve, corresponding to the plateau of the AES O/Mo curve in Figure 3. It is important to note that the amount of adsorbed oxygen, measured with these

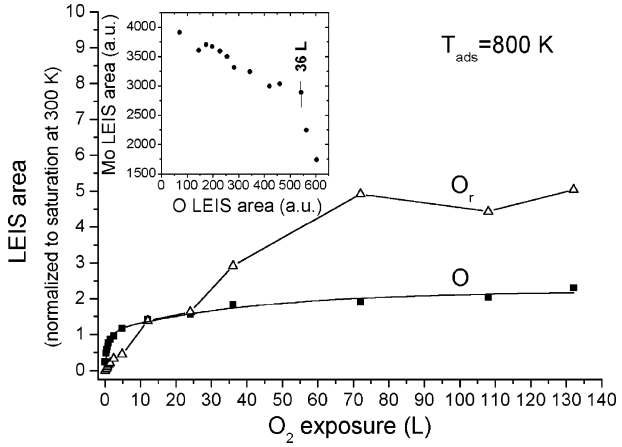

Figure 5. LEIS O and O_r peak areas, normalized to saturation at 300 K, as a function of O_2 exposure on Mo_2C/Mo(100) at 800 K. Inset: Mo LEIS area as a function of peak O area, at T_{ads} = 800 K.

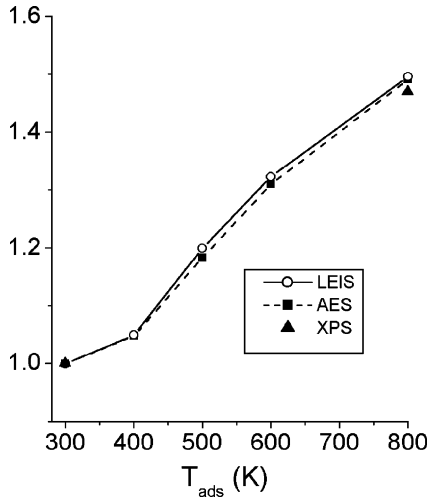

Figure 6. Saturation (relative) O signals as a function of O_2 adsorption temperature for T_{ads} = 300−600 K. Peak O area for LEIS, the O/Mo ratio for AES, and O(1s) area for XPS were displayed, all normalized to saturation at 300 K. At T_{ads} = 800 K, oxygen intensities (areas) obtained by these methods after an O_2 exposure slightly smaller than 36 L were taken into account, corresponding to the plateau of the AES O/Mo curve in Figure 3.

methods of different information depths, increases to the same extent.

To learn more about the interaction of oxygen with the carbide overlayer, detailed XPS measurements were also performed, with a θ = 23° takeoff angle. C(1s) and O(1s) windows of the spectra recorded after different O_2 treatments are presented in Figure 7. For comparison, XP peaks of the carbide surface are also shown. Up to 12 L of O_2 exposure (near saturation) at room temperature led to a small (0.1 eV) shift of the C(1s) peak toward higher binding energies, but its intensity did not change. The carbidic component of the C(1s) feature was considerably smaller at 800 K (12 L), in accordance with AES results, and it shifted to 283.0 eV. No further decrease in its intensity was observed at higher O_2 exposure (108 L) at 800 K. The carbon content of the surface was further diminished at 900 K, without any change in the peak position. At 1000 K, however, it shifted down to 282.85 eV, and the carbidic component somewhat broadened, but its area did not alter considerably. Note that the presence of oxygen did not lead to the formation of strongly perturbed C atoms, but rather small shifts of the carbidic C component occurred.

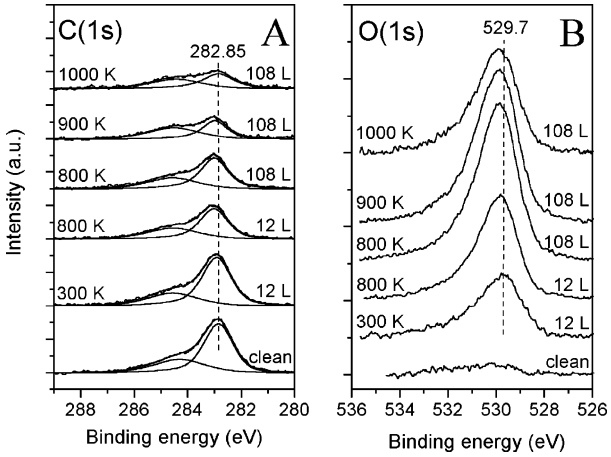

Figure 7. C(1s) and O(1s) regions of the XP spectra recorded after different O_2 treatments of Mo_2C/Mo(100), taken at θ = 23° emission angle. For comparison, the spectrum of the clean carbide surface is also displayed.

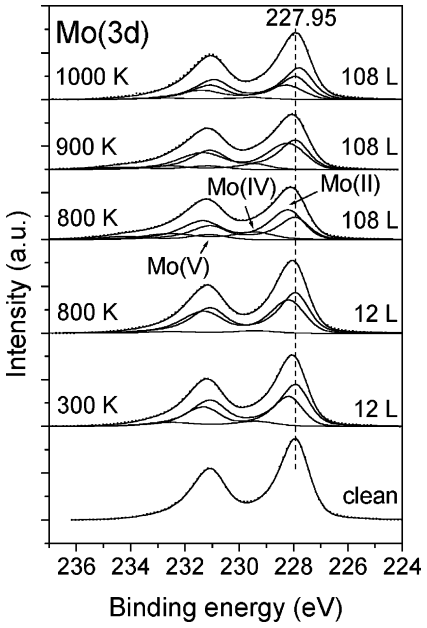

Figure 8. Mo(3d) region of the XP spectra recorded after different O_2 treatments of Mo_2C/Mo(100), taken at a θ = 23° emission angle. For comparison, the spectrum of the clean carbide surface is also displayed.

Up to 12 L of O_2 exposure (near saturation) at room temperature led to the appearance of a peak at 529.7 eV (Figure 7B), characteristic of chemisorbed (atomic) or oxidic oxygen.[24,27] Dosing the same O_2 exposure at 800 K resulted in a ∼50% enhancement of the O(1s) area (see also Figure 6) and a shift to 529.8 eV. Increasing the O_2 exposure to 108 L shifted further the O(1s) peak to 529.85 eV and caused a dramatic increase in the O(1s) intensity, in accordance with AES results (Figure 3). Note that only a slight enhancement of LEIS O intensity was observed in this exposure regime (Figure 5). The O(1s) position and area after 108 L O_2 adsorption at 900 K were almost the same. Its intensity was, however, greatly reduced at 1000 K, without any change in the position.

XPS was expected to give information about the oxidation state of molybdenum. The Mo($3d_{5/2}$) peak of the carbide surface was found at 227.95 eV (Figure 8). It could be fitted with a single doublet. Adsorption of O_2 at room temperature resulted in a small (0.1 eV) shift of the Mo($3d_{5/2}$) peak toward higher binding energies and also in some broadening. This state could

be deconvoluted into three components, a carbidic, a slightly perturbed (at 228.2 eV), and a weak, strongly perturbed contribution at 229.3 eV. The position and fwhm of the carbidic Mo(3d) component were fixed to those of the oxygen-free surface, during deconvolution. Increasing the adsorption temperature to 800 K led to similar results. Admitting a higher amount of O_2 (108 L) on the sample at 800 K caused a slight 0.05 eV shift to 228.1 eV and a pronounced broadening of the doublet toward higher binding energies, which resulted from the appearance/increase of oxidized Mo components (Mo^{II} at 228.25 eV, Mo^{IV} at 229.5 eV, and Mo^{V} at 231.1 eV). In Table 1, literature data concerning characteristic Mo($3d_{5/2}$) binding energies are summarized. With regards to the assignment of Mo^{IV} and Mo^{V} peaks, some authors claimed that the Mo(3d) doublet of Mo^{IV} in MoO_2 is split into two pairs of peaks with a 1:2 intensity ratio due to many particle effects.[24,27] The weaker component is listed as Mo^{V} in Table 1, and we use this notation, because of the similarity of the binding energy to Mo^{V}. In any case, one part of the Mo atoms was oxidized in our case at least to Mo^{IV}. Increasing the adsorption temperature to 900 K resulted in a 0.05 shift of the Mo($3d_{5/2}$) peak toward lower binding energies, caused apparently by the increase of the carbidic component in the deconvolution. At $T_{ads} = 1000$ K the position of the Mo($3d_{5/2}$) peak shifted further to 227.9 eV, which is somewhat lower than that in the clean carbide. No Mo^{V} contribution was found in the deconvolution at this temperature, and the Mo^{IV} intensity was very small as well. A new component was identified, however, at 227.8 eV, which is near to the position of metallic molybdenum.

The saturation O coverage at room temperature was estimated to be $\Theta = 0.9$ ML, based on XPS intensities taken at $\theta = 23°$ emission angle. The imfp values were calculated by the Gries equation.[45]

4. Discussion

4.1. O_2 Adsorption at 300 K. The Mo_2C/Mo(100) surface could be saturated with ~10 L of O_2 at 300 K, indicated by AES and LEIS results (Figures 3 and 4). The adsorption is dissociative, according to XPS measurements (Figure 7B). MS, AES, and XPS results show that oxygen could not remove carbon from the surface at 300 K (Figures 2, 3, and 7A). Room-temperature adsorption of O_2 did not induce significant changes in the C(1s) and Mo(3d) features (Figures 7 and 8). The slightly perturbed Mo($3d_{5/2}$) component found at 228.2 eV is near the Mo^{II} state, while the weak, strongly perturbed Mo($3d_{5/2}$) feature at 229.3 eV is close to a formal Mo^{IV} state. It is tentatively assigned to the Mo sites of the topmost layer coordinating more than one O atom. The saturation O coverage on the Mo_2C/Mo(100) surface at room temperature, estimated to be $\Theta = 0.9$ ML, is much lower than the saturation coverage on a Mo(100) metal surface ($\Theta = 1.5$ ML).[11] Carbon atoms of the topmost layer probably block one part of the oxygen adsorption centers.

An interesting feature of O_2 adsorption, followed by LEIS at 300 K, is the dramatic decrease in the C intensity (Figure 4). Note that room-temperature O_2 adsorption caused the complete elimination of the C LEIS peak of a W(100) surface covered with different amounts of carbon.[49] A similar effect was observed also on Mo(111) covered by carbon.[13] A dramatic change in the neutralization probability of the impingent ions to explain this phenomenon can be excluded, because Li^+ ions were used in those measurements. The authors assumed that O pushed C atoms to subsurface sites. We do not think it would be the case on our surface, because it would lead to a decrease in the C/Mo AES intensity, which was not observed at all. A reconstruction of the carbide surface due to the presence of oxygen, however, cannot be excluded. The decrease in the C signal can be more easily explained by the shadowing effect of O atoms located near surface C sites. In fact, XPS and valence PES studies indicated that one part of the O atoms is bound to both Mo and C atoms on the Mo_2C(0001) surface.[30] Another fraction of O atoms probably resides in the hollow sites not occupied by C.

4.2. Oxidation of the Topmost Carbide Layer. After the adsorption temperature was raised, the reaction of surface C with O to produce CO was observed from 500 K (Figure 2). Removal of surface C (Figures 3 and 7A) was accompanied by an increase in the saturation O coverage (Figures 3, 6, and 7B), very probably because in the presence of a smaller amount of surface C only a minor part of possible adsorption centers for oxygen is blocked.

We think that neither saturation at $T_{ads} \leq 600$ K nor O_2 exposures <36 L at $T_{ads} = 800$ K produce subsurface O, because O signals measured with LEIS, AES, and XPS increase simultaneously (Figure 6). O migration into the second or deeper layers would result in a larger increase in the O signals of AES and XPS, taking into account that LEIS gives information only of the topmost layer.

MS results showed that only C atoms of the first layer react with O at 800 K, and it seems that almost all carbidic carbon is removed from the outermost layer by ~36 L of O_2 exposure, because CO formation ceased up to ~20 L of O_2 exposure. In principle, it would be possible that a fraction of (carbidic) C on the first layer does not react with oxygen at 800 K; however, it should give a new peak at higher temperatures, which was not observed during the MS measurements. The graphitic contamination was found to be less reactive, or it is produced from the background after O_2 exposures, as its area in XPS measurements did not change due to O_2 treatments (Figure 7A).

4.3. Bulk Oxidation of Mo_2C/Mo(100). At higher O_2 exposures (≥36 L) at 800 K, an abrupt increase in the AES and XPS oxygen intensities occurred (Figures 3 and 7B), while the LEIS O signal did not change considerably (Figure 5). It is a clear indication of subsurface O migration. A strong gradient in the O concentration down to the information depth of XPS still remained even after 108 L of O_2 exposure at 800 K, because the ratio of the O(1s) and Mo(3d) areas was 2 times higher at $\theta = 23°$ than that at $\theta = 90°$. The migration of oxygen in the second and deeper layers led to the appearance and/or increase of oxidized (Mo^{II}, Mo^{IV}, and possibly Mo^{V}) contributions in the Mo(3d) doublet (Figure 8).

LEIS results complete our picture of this transformation at 800 K with some details of changes in the first layer. Though the O LEIS peak only slightly increased at ≥36 L, a strong decrease in the Mo signal and a break in the Mo−O curve were found (Figure 5), which means that O atoms shadow Mo sites more efficiently. It clearly indicates the occurrence of a geometrical change in the first layer. Another interesting phenomenon in LEIS measurements is the radical enhancement of the O_r peak at and above 36 L of O_2 exposure. In other words, the recoil probability of O atoms by the impingent He^+ ions is much higher after the geometric rearrangement/reconstruction of the surface. The break in the Mo−O curve is tentatively assigned to the movement of O atoms of the first layer into the on-top position, because 3D oxidation of Mo single-crystal surfaces was always accompanied by an increase in the amount of on-top O.[19−21] It seems plausible that the shadow cone of an on-top O covers a larger area than that of O in hollow sites and causes this way a stronger decrease in Mo intensity.

The removal of C from the first layer is probably an important precondition of subsurface O formation, because in the presence of C the O could not accumulate on the topmost layer at 800 K, where CO formation proceeds rapidly. 3D oxidation of the surface, set in at high O_2 exposures at 800 K, was not accompanied by an additional loss of C (Figures 3 and 7A). It suggests that C, O, and Mo are all present in the new phase, or in other words, a kind of oxycarbide was formed.

Raising the adsorption temperature to 900 K led to a decrease in the C/Mo ratios, especially in AES and XPS with $\theta = 23°$ emission angle (Table 2). It proves, in accordance with MS results, the onset of subsurface C removal, very probably through the migration of carbon to the first layer followed by its reaction with O. The comparison of the C/Mo relative intensities obtained by AES and XPS with $\theta = 23°$ and $\theta = 90°$ takeoff angles shows a strong gradient in the C concentration. At 900 K, after 108 L of O_2 exposure the oxygen signals detected by LEIS, AES, and XPS did not differ much from those obtained at 800 K, indicating a similar amount of O in the surface region and also a similar distribution of oxygen. Accordingly, the Mo(3d) doublet resembled very much of that found at 800 K, suggesting the same oxidation states of molybdenum.

However, oxygen intensities in AES and XPS detected at 1000 K were much smaller. It is probably the consequence of the higher diffusion rate of C at this temperature, supplying continuously the reaction partner for O on the topmost layer. Interestingly, the comparison of the C/Mo relative intensities obtained by AES and XPS at 1000 K (Table 2) shows the diminution of the C concentration gradient, which is probably a consequence of the higher carbon mobility as well. In accordance with the decrease in the amount of adsorbed oxygen, the C(1s) peak shifted toward lower binding energies at 1000 K (Figure 7A). Similarly, the highly oxidized (Mo^{IV} and Mo^{V}) components in the Mo(3d) doublet almost disappeared, and the intensity of Mo^{II} state also diminished. Moreover, a new component appeared at the position near the metallic state. The latter feature is assigned to Mo atoms in C and O depleted environment. We do not think that there are large volumes of metallic Mo in the sample. Instead, C and O are probably dispersed in the whole surface region. Quite a large number of Mo sites coordinating neither C nor O atoms, however, can exist, giving the metal-like component in the Mo(3d) doublet.

After 900 K adsorption, an apparent increase in the carbidic Mo(3d) component was observed (Figure 8), while the C content of the sample decreased. It was probably the consequence of two contradictory effects. The C consumption tends to shift down the peak position, while the oxygen content leads to a shift toward higher binding energies. The deconvolution procedure is unable to distinguish between pure carbidic Mo in a Mo_2C environment and certain Mo atoms coordinating few C and few O atoms.

5. Conclusion

(i) It was shown by angle-resolved XPS measurements that a Mo_2C overlayer with a homogeneous C distribution down to the information depth of XPS, estimated to be 5.7 nm, was produced on Mo(100) by repeating C_2H_4 adsorption at 900 K and annealing in a vacuum to 1265 K.

(ii) O_2 adsorbs dissociatively on the carbide layer at room temperature. One part of the chemisorbed oxygen is bound to both C and Mo sites, indicated by LEIS. Another fraction of oxygen atoms probably resides in the hollow sites not occupied by C.

(iii) The reaction of oxygen with C atoms of the topmost layer to produce CO was observed from $T_{ads} = 500$ K. The removal of surface C resulted in an increase in the saturation O coverage, but all adsorbed oxygen atoms are located on the topmost layer up to $T_{ads} = 600$ K and even at small O_2 exposures at 800 K. At higher exposures at 800 K, the migration of O to subsurface sites sets in, forming this way a kind of oxycarbide, characterized by oxidized Mo states. It was accompanied by some rearrangement/reconstruction of the topmost layer, indicated by LEIS, but the amount of O on the first layer did not alter.

(iv) The removal of carbon atoms from subsurface sites by oxygen starts at $T_{ads} = 900$ K. A strong gradient in the C concentration was observed at this temperature, which is attenuated at 1000 K, probably due to the larger diffusion rate of C. The amount of adsorbed O at 1000 K is greatly reduced as well, which is also rationalized by the higher C mobility.

Acknowledgment. This work was supported by grants OTKA D38489, TS40877, and T46351.

References and Notes

(1) Zhang, Y.; Ichihashi, T.; Landree, E.; Nihey, F.; Lijima, S. *Science* **1999**, *285*, 1719.
(2) Nakajima, T.; Shirasaki, T. *J. Electrochem. Soc.* **1997**, *144*, 2096.
(3) Levy, R. L.; Boudart, M. *Science* **1973**, *181*, 547.
(4) Oyama, S. T. *Catal. Today* **1992**, *15*, 179.
(5) Chen, J. G. *Chem. Rev.* **1996**, *96*, 1477 and references therein.
(6) Solymosi, F.; Cserényi, J.; Szöke, A.; Bánsági, T.; Oszkó, A. *J. Catal.* **1997**, *165*, 150.
(7) Solymosi, F.; Németh, R.; Óvári, L.; Egri, L. *J. Catal.* **2000**, *195*, 316.
(8) Shu, Y.; Ichikawa, M. *Catal. Today* **2001**, *71*, 55 and references therein.
(9) Delporte, P.; Meunier, F.; Pham-Huu, C.; Vennegues, P.; Ledoux, M. J.; Guille, J. *Catal. Today* **1995**, *23*, 251.
(10) Guillot, C.; Riwan, R.; Lecante, J. *Surf. Sci.* **1976**, *59*, 581.
(11) Ko, E. I.; Madix, R. J. *Surf. Sci.* **1981**, *109*, 221.
(12) Schöberl, Th. *Surf. Sci.* **1995**, *327*, 285.
(13) Overbury, S. H. *Surf. Sci.* **1987**, *184*, 319.
(14) Frühberger, B.; Chen, J. G. *Surf. Sci.* **1995**, *342*, 38.
(15) Frühberger, B.; Chen, J. G.; Eng, J., Jr.; Bent, B. E. *J. Vac. Sci. Technol., A* **1996**, *14*, 1475.
(16) Ollis, D. F.; Boudart, M. *Surf. Sci.* **1970**, *23*, 320.
(17) Jentz, D.; Rizzi, S.; Barbieri, A.; Kelly, D.; Van hove, M. A.; Somorjai, G. A. *Surf. Sci.* **1995**, *329*, 14.
(18) Overbury, S. H.; Stair, P. C. *J. Vac. Sci. Technol., A* **1983**, *1*, 1055.
(19) Stefanov, P. K.; Marinova, Ts. S. *Surf. Sci.* **1988**, *200*, 26.
(20) Colaianni, M. L.; Chen, J. G.; Weinberg, W. H.; Yates, J. T., Jr. *Surf. Sci.* **1992**, *279*, 211.
(21) Kim, S. H.; Stair, P. C. *Surf. Sci.* **2000**, *457*, L347 and references therein.
(22) Santra, A. K.; Min, B. K.; Goodman, D. W. *Surf. Sci.* **2002**, *513*, L441.
(23) Schroeder, T.; Giorgi, J. B.; Hammoudeh, A.; Magg, N.; Bäumer, M.; Freund, H.-J. *Phys. Rev B.* **2002**, *65*, 115411.
(24) Schroeder, T.; Zegenhagen, J.; Magg, N.; Immaraporn, B.; Freund, H.-J. *Surf. Sci.* **2004**, *552*, 85.
(25) Grant, J. L.; Fryberger, T. B.; Stair, P. C. *Surf. Sci.* **1985**, *159*, 333.
(26) Minni, E.; Werfel, F. *Surf. Interface Anal.* **1988**, *12*, 385.
(27) Brox, B.; Olefjord, I. *Surf. Interface Anal.* **1988**, *13*, 3.
(28) McIntyre, N. S.; Johnston, D. D.; Coatsworth, L. L.; Davidson, R. D.; Brown, J. R. *Surf. Interface Anal.* **1990**, *15*, 265.
(29) Smuddle, G. H.; Stair, P. C. *Surf. Sci.* **1994**, *317*, 65.
(30) Edamoto, K.; Sugihara, M.; Ozawa, K.; Otani, S. *Surf. Sci.* **2004**, *561*, 101.
(31) St. Clair, T. P.; Oyama, S. T.; Cox, D. F. *Surf. Sci.* **2000**, *468*, 62.
(32) Solymosi, F.; Oszkó, A.; Bánsági, T.; Tolmacsov, P. *J. Phys. Chem. B* **2002**, *106*, 9613.
(33) Bugyi, L.; Oszkó, A.; Solymosi, F. *Surf. Sci.* **2000**, *461*, 177.
(34) Óvári, L.; Kiss, J.; Farkas, A. P.; Solymosi, F. *Surf. Sci.* **2004**, *566*−*568*, 1082.
(35) Brainard, W. A.; Wheeler, D. R. *J. Vac. Sci. Technol.* **1978**, *15*, 1800.
(36) Reinke, P.; Oelhafen, P. *Diamond Relat. Mater.* **1999**, *8*, 155.
(37) Sugihara, M.; Ozawa, K.; Edamoto, K.; Otani, S. *Solid State Commun.* **2002**, *121*, 1.

(38) St. Clair, T. P.; Oyama, S. T.; Cox, D. F.; Otani, S.; Ishizawa, Y.; Lo, R. L.; Fukui, K. I.; Iwasawa, Y. *Surf. Sci.* **1999**, *426*, 187.
(39) Clayton, C. R.; Lu, Y. C. *Surf. Interface Anal.* **1989**, *14*, 66.
(40) Zingg, D. S.; Makovsky, L. E.; Tisher, R. E.; Brown, F. R.; Hercules, D. M. *J. Phys. Chem.* **1980**, *84*, 2898.
(41) Di Giuseppe, G.; Selman, J. R. *J. Electroanal. Chem.* **2003**, *559*, 31.
(42) Scofield, J. H. *J. Electron Spectrosc. Relat. Phenom.* **1976**, *8*, 129.
(43) Shirley, D. A. *Phys. Rev. B* **1972**, *5*, 4709.
(44) Kövér, L.; Cserny, I.; Brabec, V.; Fi×f0er, M.; Dragoun, O.; Novák, J. *Phys. Rev. B* **1990**, *42*, 643 and references therein.
(45) Gries, W. H. *Surf. Interface Anal.* **1996**, *24*, 38.
(46) Tanuma, S.; Powell, C. J.; Penn, D. R. *Surf. Interface Anal.* **1994**, *21*, 165.
(47) Fukui, K. I.; Lo, R. L.; Otani, S.; Iwasawa,Y. *Chem. Phys. Lett.* **2000**, *325*, 275.
(48) Bugyi, L.; Solymosi, F. *J. Phys. Chem. B* **2001**, *105*, 4337.
(49) Mullins, D. R.; Overbury, S. H. *Surf. Sci.* **1989**, *210*, 501.